Available online at www.sciencedirect.com
ScienceDirect
Trans. Nonferrous Met. Soc. China 32(2022) 1253−1260
Transactions of Nonferrous Metals Society of China
www.tnmsc.cn

Hierarchical porous Co_3O_4 spheres fabricated by modified solvothermal method as anode material in Li-ion batteries

Yan FENG[1,2], Cai-yu CAO[1,2], Jing ZENG[3], Ri-chu WANG[1,2], Chao-qun PENG[1,2], Xiao-feng WANG[1,2]

1. School of Materials Science and Engineering, Central South University, Changsha 410083, China;
2. Hunan Provincial Key Laboratory of Electronic Packaging and Advanced Functional Materials, Changsha 410083, China;
3. School of Metallurgy and Environment, Central South University, Changsha 410083, China

Received 7 February 2021; accepted 9 January 2022

Abstract: Hierarchical porous Co_3O_4 spheres were synthesized by a solvothermal method followed by high-temperature calcination. XRD, SEM, TEM and electrochemical tests were used to study the structure and performance of the hierarchical porous Co_3O_4 spheres. The results show that the Co_3O_4 synthesized at a calcination temperature of 700 °C (Co_3O_4-700) is micro-sized spheres (1−2 μm) consisting of plentiful nanoparticles (50−200 nm) and numerous pores (~100 nm). Due to its numerous porous morphology, the Co_3O_4-700 anode exhibits the highest cycling performance with excellent reversible discharge and charge specific capacities of 745 and 755 mA·h/g at the current density of 100 mA/g after 100 charge−discharge cycles, respectively.

Key words: Co_3O_4; lithium-ion batteries; porous structure; spheres; calcination

1 Introduction

Nowadays, lithium-ion batteries (LIBs) have been applied in all aspects of life due to the continuous exhaustion of non-renewable fossil energy. With the rapid development of portable devices (mobile phones, computers, etc.) and electric vehicles, it is urgent to explore for the high-powered and stable anode materials for LIBs [1−3]. Graphite [4] is the conventional anode material, whose theoretical specific capacity is much lower than that of transition metal oxides (FeO_x [5,6], MnO_x [7,8], CoO_x (Co_3O_4, 890 mA·h/g) [9−11], and SnO [12,13] etc.). Among these, Co_3O_4 is widely regarded as a potential anode candidate material on account of its high theoretical specific capacity, natural abundance and excellent electrochemical performance (accommodating 8 lithium atoms per unit) [11]. However, the large volume expansion and poor electrical conductivity of Co_3O_4 anode cause inferior cycling properties. Shortening the size of particles and preparing porous structure are two effective methods to solve these problems. The nanoparticles increase the contact area of electrode and electrolyte, shorten the Li^+ transport channel, thus enhancing the electrochemical properties of anodes [14]. However, the nanoparticles are easy to agglomerate, which causes the pulverization of the electrode [15,16]. The porous structures, which provide the accommodation for repeated Li^+ intercalation/deintercalation, also play a role in solving volume expansion and strengthening electrochemical stability [17]. Various strategies are used to prepare mesoporous Co_3O_4. For example, LI et al [18] used a ligand (4,5-imidazole-dicarboxylic acid) to prepare nanostructure precursor (1D), and finally

Corresponding author: Xiao-feng WANG, E-mail: 1wangxiaofeng@163.com
DOI: 10.1016/S1003-6326(22)65871-0

obtained mesoporous Co_3O_4/NC nanowires. SHIN and LEE [19] synthesized mesoporous Co_3O_4 hollow spheres using their preparation carbon sphere@Co-glycolate as precursor. LI et al [20] synthesized mesoporous Co_3O_4 by a spray pyrolysis process using $CoCl_2·6H_2O$ as the precursor in oxygen atmosphere, which showed a high specific capacity (1340 mA·h/g after 50 cycles at 200 mA/g). A hierarchical structure, nano/microstructure, is proposed to efficiently reduce the agglomeration of nanoparticles and prepare the porous structure. Nowadays, no research reported the control of the size of pores by solvothermal method combined the calcination, which is low-cost and uncomplex.

In this work, a modified solvothermal method followed by a high-temperature treatment was utilized to control the pores' size of Co_3O_4 and therefore enhance its electrochemical stability. The microstructures and phases of the synthesized porous Co_3O_4 were investigated by XRD, SEM, and TEM. The influence of microstructure on charge and discharge performance was characterized by electrochemical tests.

2 Experimental

2.1 Synthesis of $CoCO_3$ and Co_3O_4

2.1.1 Synthesis of micro-sized spherical $CoCO_3$

0.476 g cobalt chloride ($CoCl_2·6H_2O$) and 3.95 g ammonium bicarbonate (NH_4HCO_3) were added to 60 mL 1,2-propanediol. The solution was stirred with a magnetic stirrer and then transferred to a 100 mL Teflon-lined stainless steel autoclave and placed at 190 °C for 20 h. The products after centrifugation were kept at 60 °C for 12 h in the blast drying box. The pink $CoCO_3$ powder was obtained.

2.1.2 Synthesis of hierarchical porous Co_3O_4

The gained $CoCO_3$ powder was placed equably in a ceramic crucible, heated from room temperature to 500 and 700 °C and kept for 5 h, respectively. When the oven was cooled, black powders were obtained. The powders conciliated at 500 and 700 °C were noted as Co_3O_4-500 and Co_3O_4-700, respectively.

2.2 Materials characterization

The chemical compositions of $CoCO_3$ and Co_3O_4 powders were characterized using the X-ray diffraction (XRD) experiment on Rigaku D/max 2500 (λ=0.15405 nm). The samples were scanned at a speed of 8 (°)/min and 2θ values from 5° to 80° to obtain the XRD patterns, which should be compared with the standard PDF card. A Fourier transform infrared (FTIR) pattern was received using a Nicolet Nexus 670 FTIR spectrometer. The microstructure patterns of micro-sized spherical $CoCO_3$ and micro/nano-sized Co_3O_4 were obtained on the scanning electron microscope (SEM, Nano SEM 230, FEI, America). The transmission electron microscope (TEM, Tecnai G2 F20, FEI, America) revealed the inner crystal structure of Co_3O_4 and $CoCO_3$ powders.

2.3 Electrochemical tests

The slurry was composed of the active material (pure Co_3O_4, 70 wt.%), conductive agent (acetylene black, 20 wt.%) and binder (polyvinylidene fluoride, 10 wt.%). This slurry was coated evenly on the copper clad, dried at 110 °C for 12 h. The three-component electrolyte was composited by ethylene carbonate (EC), diethylene carbonate (DEC) and dimethyl carbonate (DMC) in the same volume. A cyclic voltammogram (CV) curve was characterized on an electrochemical workstation (CHI604E). The parameters were set at the voltage of 0.01−3 V and the scanning speed of 0.1 mV/s. A galvanostatic charging and discharging process characterized the cyclic performance of anodes on the Land automatic battery tester (CT2001A, Wuhan, China). The voltage range was identical to the parameter of CV curve. The charge transfer property of Co_3O_4-500 and Co_3O_4-700 anodes was analyzed by electrochemical impendence spectroscopy (EIS, IM6ex) measurement. The parameters were set at the frequency of 100 kHz−10 mHz and the scanning speed of 0.5 mV/s.

3 Results and discussion

3.1 Phase component and microstructure

Figure 1 illustrates the XRD patterns of precursor $CoCO_3$ and synthesized Co_3O_4-500 and Co_3O_4-700. The peaks of Co_3O_4-500 and Co_3O_4-700 are located at 2θ values of 31°, 36° and 38°, corresponding to the (220), (311) and (400) planes of the standard Co_3O_4, which confirms the successful preparation of the pure Co_3O_4-500 and

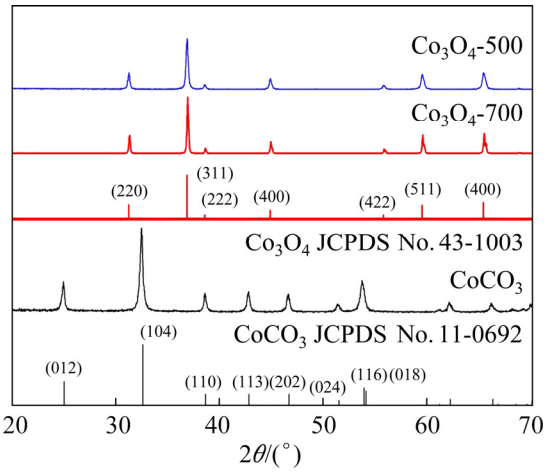

Fig. 1 XRD patterns of micro-sized $CoCO_3$ and hierarchical porous Co_3O_4-500 and Co_3O_4-700

Co_3O_4-700. The peak of Co_3O_4-700 located at 2θ values of 36° is visibly sharper than that of Co_3O_4-500, which illustrates high crystallinity. The peaks of $CoCO_3$ at 2θ values of 25°, 32° and 38° correspond to the planes (012), (104) and (110), respectively [11,21]. The XRD results display that $CoCO_3$, Co_3O_4-500 and Co_3O_4-700 powders are obtained without any impurities.

The SEM images were utilized to characterize morphologies of $CoCO_3$, Co_3O_4-500 and Co_3O_4-700. Figures 2(a, b) demonstrate that the morphology of $CoCO_3$ powders is composed of micro-sized spheres (1−2 μm) and nano-sized platelike surface. Co_3O_4-500 and Co_3O_4-700 powders consist of micro-sized spheres similar to those $CoCO_3$ powders. These micro-sized spheres of Co_3O_4-500 and Co_3O_4-700 comprise nanoparticles and pores as shown in Figs. 2(c−f). The nanoparticles and pores of Co_3O_4 are derived from the escape of carbon dioxide in $CoCO_3$ during the heat treatment process [15]. The pores size (~100 nm) of Co_3O_4-700 is obviously larger than that of Co_3O_4-500. The reason for the growth of nanoparticles is the adsorption of the monomer from the small curvature nanoparticles, which are derived from the dissolution of the large curvature nanoparticles in the process of high-temperature calcination according to the Ostwald ripening mechanism [22]. As these nanoparticles grow, the pores size of Co_3O_4 increases.

Furthermore, the TEM and HRTEM images are used for further characterizing the micro-structure of Co_3O_4-700. As for Co_3O_4-700, its particle size is about 2 μm, which consists of nanoparticles (50−200 nm) and numerous pores,

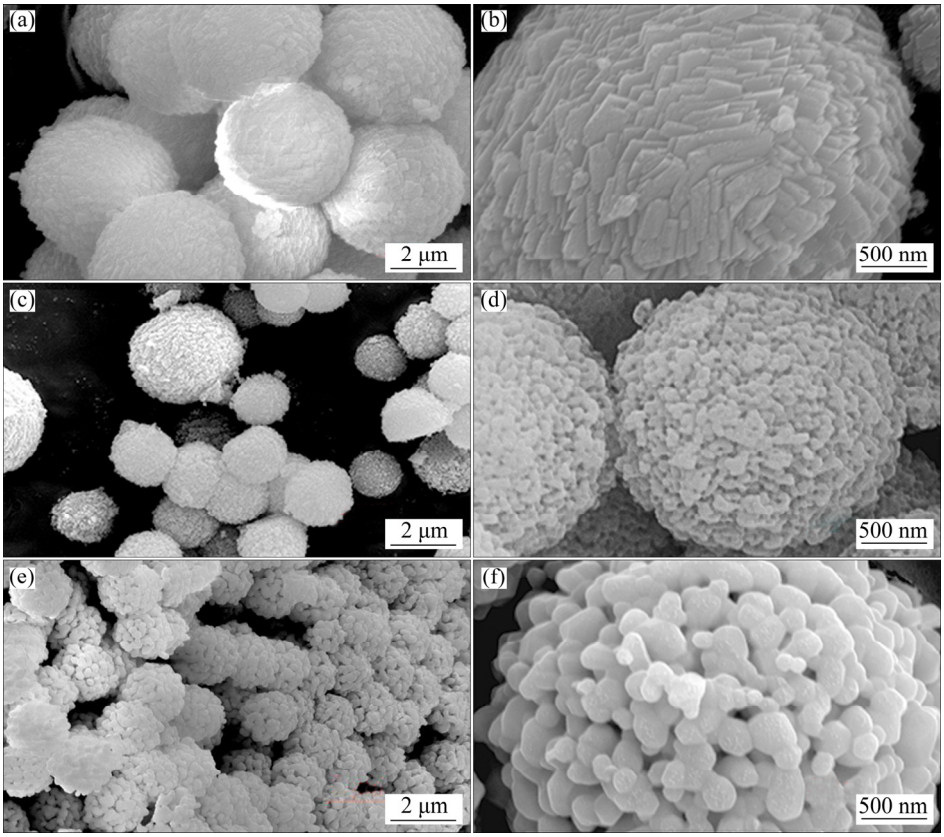

Fig. 2 SEM images of micro-sized $CoCO_3$ (a, b), and hierarchical porous Co_3O_4-500 (c, d) and Co_3O_4-700 (e, f)

well-matching with the SEM images as displayed in Fig. 3(a). The HRTEM image shows that lattice fringe of hierarchical porous Co_3O_4-700 is 0.47 nm matching to (111) plane as manifested in Fig. 3(b).

3.2 Electrochemical performance

Electrochemical tests were utilized for characterizing the effect of unique morphology on electrochemical properties. The first three CV curves of Co_3O_4-500 and Co_3O_4-700 anodes are demonstrated in Figs. 4(a, b). The peaks of Co_3O_4-500 and Co_3O_4-700 located at 0.855 and 0.852 V are corresponding to the reduction conversion process from Co^{3+} and Co^{2+} into Co (Reaction (1)) in the first anodic curve, respectively [22]. The corresponding oxidation peaks appear at 2.057 and 1.949 V, indicating that Co has converted to CoO (Reaction (2)),

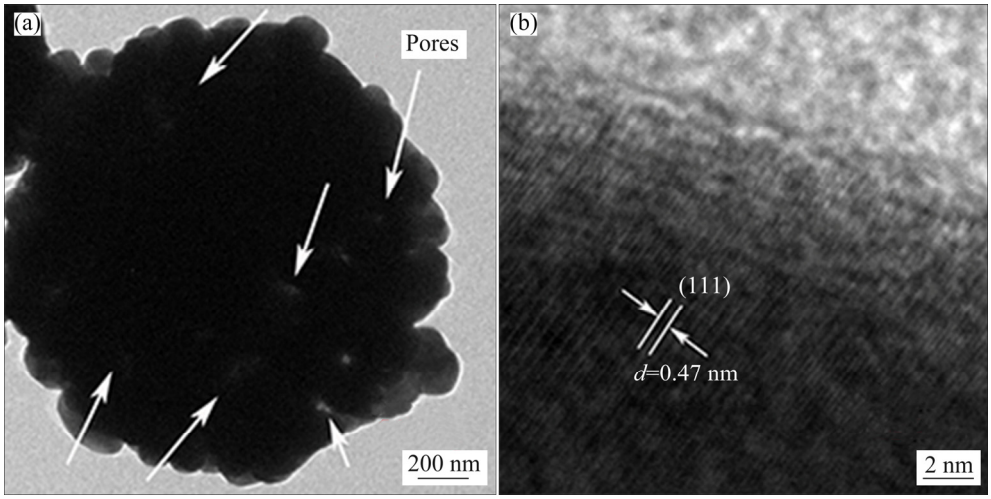

Fig. 3 TEM (a) and HRTEM (b) images of hierarchical porous Co_3O_4-700

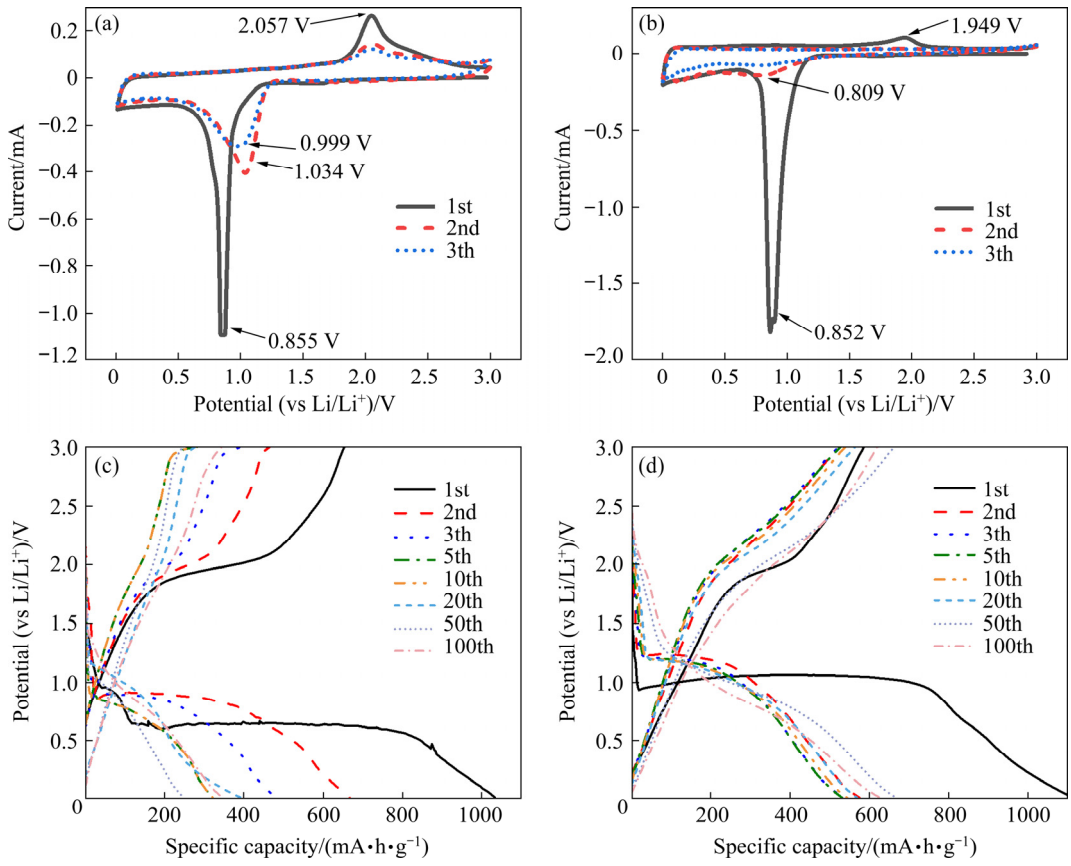

Fig. 4 The first three CV curves of Co_3O_4-500 (a) and Co_3O_4-700 (b), and charge−discharge profiles of Co_3O_4-500 (c) and Co_3O_4-700 (d)

respectively [23]. Among these three curves, the first curve distinguishes from the other curves, deriving from the formation of a solid electrolyte interface (SEI) film. The well overlapping of other curves indicates the reversible transformation between Co and CoO. The oxidation peak activity of CO_3O_4-500 located at 2.057 V is significantly greater than that of Co_3O_4-700 located at 1.949 V because small size nanoparticle increases the contact area between electrode and electrolyte. The voltage variation of the Co_3O_4-500 and Co_3O_4-700 anodes is consistent with the CV curve in the current charge−discharge voltage file of 500 mA/g shown in Figs. 4(c, d). The platforms of Co_3O_4-700 located at 0.88 and 1.95 V correspond to the reversible conversion reactions between cobalt oxide and cobalt as displayed in Fig. 4(d). Compared with that of Co_3O_4-500, the overlapping of Co_3O_4-700 anode is higher after 100 charge−discharge processes, and the chemical reaction of Co_3O_4-700 anode is more invertible, which explains that the effect of pores size on electrochemical performance is greater than that of grains size.

$$Co_3O_4+8Li=3Co+4Li_2O \quad (1)$$

$$Co+Li_2O=CoO+2Li \quad (2)$$

Figure 5(a) illustrates the cyclic properties of Co_3O_4-500 and Co_3O_4-700 at 100 mA/g. In the 1st cycle, the discharge capacity of Co_3O_4-500 and Co_3O_4-700 is 1416 and 1095.5 mA·h/g, respectively. The specific capacity of Co_3O_4-500 is higher than Co_3O_4-700 due to Co_3O_4 nanoparticles, which improves the specific surface of the particle and increases the contact area between electrode and electrolyte (Fig. 3(a)) [21]. The capacity attenuation is due to the formation of SEI films and electrolyte decomposition in the 1st stage as shown in Fig. 5(a) [24]. Co_3O_4-700 anode has higher reversible discharge and charge capacities of 745 and 755 mA·h/g than those (529 and 526 mA·h/g) of Co_3O_4-500 due to its large pores size, which increases the length of lithium-ion transmission path [25]. After long-term cycles, the discharge capacity of Co_3O_4-700 remains 230 mA·h/g at a large current density (2000 mA/g) as displayed in Fig. 5(b), which exhibits excellent cycling stability. More significantly, when the current densities are set to be 50, 100, 200, 300, 500 and 1000 mA/g, the capacities of Co_3O_4-700 anode are 599.4, 507.9, 474.6, 499.5, 482.9 and 399.6 mA·h/g, respectively.

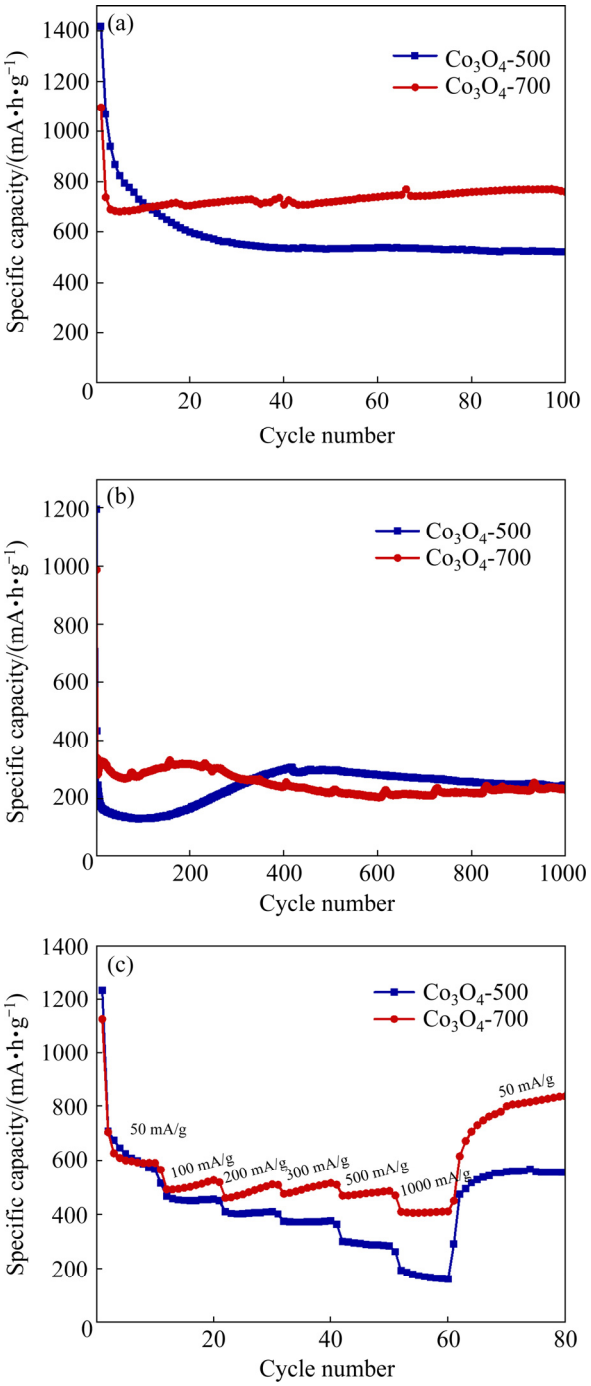

Fig. 5 Cyclic property of 100 mA/g (a), long cycle performance at 2000 mA/g (b), and rate property (c) of hierarchical porous Co_3O_4-500 and Co_3O_4-700

The capacity of Co_3O_4-700 anode recovers to 818.6 mA·h/g when the current density returns to 50 mA/g as demonstrated in Fig. 5(c). JING et al [26] synthesized the microflow Co_3O_4, whose porous structure provides charge storage space. Therefore, the microflow Co_3O_4 has excellent rate performance (The capacity of Co_3O_4 anode recovers

to 765 mA·h/g when the current density returns to 200 mA/g). Co_3O_4-500 and Co_3O_4-700 lie in the size of the nanoparticles and the pores. Compared with Co_3O_4-500, the larger nanoparticle size of Co_3O_4-700 is not conducive to the increase of the contact area between electrode and electrolyte, but it has better cycling performance. It is obvious that the rate performance of Co_3O_4-700 is superior to that of Co_3O_4-500, which illustrates that the large pore size is an important influence factor on the rate performance. MULE et al [27] synthesized porous structure on nickel plate, resulting in excellent rate performance. Table 1 shows the comparison of the cycling properties of Co_3O_4-based anodes at 100 mA/g.

Table 1 Comparison of cyclic properties of Co_3O_4-based anodes

Active material	Current density/ ($mA·g^{-1}$)	Specific capacity/ ($mA·h·g^{-1}$)	Cycle number	Ref.
Co_3O_4 nanotube	250	856.4	60	[28]
Graphene-embedded Co_3O_4	100	990.8	100	[10]
Co_3O_4 /Ni	100	748.7	100	[10]
Flower-like SnS_2/Co_3O_4	100	715	100	[29]
Co_3O_4 nanoparticles	50	585.6	200	[30]
Hierarchical porous Co_3O_4-700	100	755	120	This work

EIS measurement was utilized to observe the conductivity and charge transfer properties of Co_3O_4-500 and Co_3O_4-700 anodes (Fig. 6). The Nyquist plot is divided into two parts (a semicircle and a line). The semicircle represents the region of high frequency, which is determined by the resistance of charge transfer (R_{ct}) and the impedance of SEI films; the straight line shows the region of low frequency formed by lithium-ion diffusion [31,32]. The R_{ct} of Co_3O_4-700 anode is about 290 Ω, and R_{ct} of Co_3O_4-500 anode is about 670 Ω as displayed in Fig. 6. The R_{ct} of Co_3O_4-700 anode is evidently small as hierarchical porous structure shortens the lithium-ion transport channel. This suggests that hierarchical porous Co_3O_4-700 anode has excellent charge transfer property.

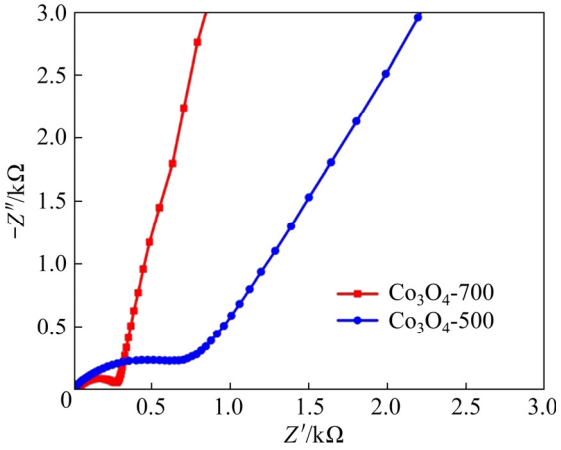

Fig. 6 Nyquist diagrams of hierarchical porous Co_3O_4-500 and Co_3O_4-700

4 Conclusions

(1) Hierarchical porous Co_3O_4 spheres were prepared via a solvothermal method combined with heat treatment. The micro-sized (1−2 μm) spheres of Co_3O_4-700 consist of nano-sized (50−200 nm) particles. The hierarchical morphology increases the contact area of electrode and electrolyte, weakens the aggregation of nanoparticles and relieves the volume expansion.

(2) The unique morphology and reversible reactions result in excellent electrochemical stability. Specifically, a reversible specific capacity (755 mA·h/g) of Co_3O_4-700 is achieved when the current density is 100 mA/g after 100 charge−discharge cycles. The specific capacity of Co_3O_4-700 anode recovers to 818.6 mA·h/g when the current density backs to 50 mA/g, which manifests superior rate property.

Acknowledgments

The authors appreciate Prof. Jun LIU and his team from Central South University for their kind help and support in the electrochemical tests. The research was funded by the Natural Science Foundation of Hunan Province, China (No. 2020JJ4729).

References

[1] WANG Li, FU Yuan-yuan, CHEN Ya-qin, LI Yan-fei, ZHOU Ri-hui, CHEN Shou-hui, SONG Yong-hai. Ultralight flower ball-like Co_3O_4/melamine-derived carbon foam as anode materials for lithium-ion batteries [J]. Journal of Alloys and Compounds, 2017, 724: 1117−1123.

[2] ZENG Gui-lin, ZHOU Wei, ZHENG Jia-ling, FAN Zhan-hua, CHEN Han. Synthesis of hollow carbon microspheres with tunable shell numbers for high-performance anode material in lithium-ion batteries [J]. Journal of Nanoscience and Nanotechnology, 2020, 20: 4899−4906.

[3] WANG Bin, WANG Shi-feng, TANG Yuan-yuan, JI Ya-xiong, LIU Wei, LU Xiao-ying. Hydrothermal synthesis of mesoporous Co_3O_4 nanorods as high capacity anode materials for lithium ion batteries [J]. Energy Procedia, 2019, 158: 5293−5298.

[4] ZHOU Kai-qiang, LAI Lan-fang, ZHEN Yi-chao, HONG Zhen-sheng, GUO Ju-hua, HUANG Zhi-gao. Rational design of Co_3O_4/Co/carbon nanocages composites from metal organic frameworks as an advanced lithium-ion battery anode [J]. Chemical Engineering Journal, 2017, 316: 137−145.

[5] JIANG Tian-cai, BU Fan-xing, FENG Xiao-xiang, SHAKIR I, HAO Guo-lin, XU Yu-xi. Porous Fe_2O_3 nanoframeworks encapsulated within three-dimensional graphene as high-performance flexible anode for lithium-ion battery [J]. ACS Nano, 2017, 11: 5140−5147.

[6] ZHANG Qiang, HUANG Ning, HUANG Zhen, CAI Liang-ting, WU Jing-hua, YAO Xia-yin. CNTs@S composite as cathode for all-solid-state lithium-sulfur batteries with ultralong cycle life [J]. Journal of Energy Chemistry, 2020, 40: 151−155.

[7] ZHU Qian-cheng, HU Hao, LI Guo-jian, ZHU Chen-bo, YU Ying. TiO_2 nanotube arrays grafted with MnO_2 nanosheets as high-performance anode for lithium ion battery [J]. Electrochimica Acta, 2015, 156: 252−260.

[8] DENG Shuo, WANG Lu, HOU Ting-jun, LI Y Y. Two-dimensional MnO_2 as a better cathode material for lithium ion batteries [J]. The Journal of Physical Chemistry C, 2015, 119: 28783−28788.

[9] LIU Yan-guo, CHENG Zhi-ying, SUN Hong-yu, ARANDIYAN H, LI Jin-peng, AHMAD M. Mesoporous Co_3O_4 sheets/3D graphene networks nanohybrids for high-performance sodium-ion battery anode [J]. Journal of Power Sources, 2015, 273: 878−884.

[10] JING Ming-jun, ZHOU Min-jie, LI Gang-yong, CHEN Zhen-gu, XU Wenyuan, CHEN Xiao-bo, HOU Zhao-hui. Graphene-embedded Co_3O_4 rose-spheres for enhanced performance in lithium ion batteries [J]. ACS Applied Materials & Interfaces, 2017, 9: 9662−9668.

[11] WANG Zheng-dong, QU Shao-hua, CHENG Yong-hong, ZHENG Cheng-hui, CHEN Si-yu, WU Hong-jing. Facile synthesis of Co_3O_4 spheres and their unexpected high specific discharge capacity for lithium-ion batteries [J]. Applied Surface Science, 2017, 416: 338−343.

[12] ZENG Jing, PENG Chao-qun, WANG Ri-chu, LIU Ya-jing, WANG Xiao-feng, LIU Jun. Large-scale synthesis of hierarchical SnO spheres assisted with poly (N-isopropylacrylamide) for high lithium storage capacity [J]. Ceramics International, 2019, 45: 1246−1250.

[13] ZENG Jing, PENG Chao-qun, WANG Ri-chu, LIU Ya-jing, CAO Cai-yu, WANG Xiao-feng, LIU Jun. SnO@amorphous TiO_2 core-shell composite for advanced lithium storage [J]. Ceramics International, 2019, 45: 19404−19408.

[14] LIU Wen-bin, FU Yuan-yuan, LI Yan-fei, CHEN Shou-hui, SONG Yong-hai, WANG Li. Three-dimensional carbon foam surrounded by carbon nanotubes and Co−Co_3O_4 nanoparticles for stable lithium-ion batteries [J]. Composites Part B: Engineering, 2019, 163: 464−470.

[15] HUANG Guo-yong, XU Sheng-ming, LU Sha-sha, LI Lin-yan, SUN Hong-yu. Micro-/nanostructured Co_3O_4 anode with enhanced rate capability for lithium-ion batteries [J]. ACS Applied Materials & Interfaces, 2014, 6: 7236−7243.

[16] WANG Yuan-yu, ZHU Wen-jun. Micro/nano-structured $Li_4Ti_5O_{12}$ as high rate anode material for lithium ion batteries [J]. Solid State Ionics, 2020, 349: 115297.

[17] TONG Xiao-ling, ZENG Min, LI Jing, LIU Zhan-jun. Porous Co_3O_4@TiO_2 core-shell nanofibers as advanced anodes for lithium ion batteries [J]. Journal of Alloys and Compounds, 2017, 723: 129−138.

[18] LI Li-xin, DONG Guang-sheng, XU Ying-ming, CHENG Xiao-li, GAO Shan, ZHANG Xian-fa, ZHAO Hui, HUO Li-hua. H3IDC-assisted synthesis of mesoporous ultrafine Co_3O_4/N-doped carbon nanowires as a high rate and long-life anode for Lithium-ion batteries [J]. Journal of Alloys and Compounds, 2020, 818: 152826.

[19] SHIN H, LEE W J. Ultrathin mesoporous shell Co_3O_4 hollow spheres as high-performance electrode materials for lithium-ion batteries [J]. Materials Chemistry and Physics, 2018, 214: 165−171.

[20] LI Tao, LI Xin-hai, WANG Zhi-xing, GUO Hua-jun, HU Qi-yang, PENG Wen-jie. Synthesis of nanoparticles-assembled Co_3O_4 microspheres as anodes for Li-ion batteries by spray pyrolysis of $CoCl_2$ solution [J]. Electrochimica Acta, 2016, 209: 456−463.

[21] YANG Tao, LIU Yan-gai, HUANG Zhao-hui, YANG Qian, GUAN Ming, FANG Ming-hao, WU Xiao-wen. A facile strategy for fabricating hierarchically mesoporous Co_3O_4 urchins and bundles and their application in Li-ion batteries with high electrochemical performance [J]. RSC Advances, 2015, 5: 24486−24493.

[22] ZHAN Liang, CHEN Hong-bin, FANG Jun-qi, WANG Su-qing, DING Liang-xin, LI Zhong, ASHMAN P J, WANG Hai-hui. Coaxial Co_3O_4@polypyrrole core-shell nanowire arrays for high performance lithium ion batteries [J]. Electrochimica Acta, 2016, 209: 192−200.

[23] WON J M, CHO J S, KANG Y C. Superior electrochemical properties of SiO_2-doped Co_3O_4 hollow nanospheres obtained through nanoscale Kirkendall diffusion for lithium-ion batteries [J]. Journal of Alloys and Compounds, 2016, 680: 366−372.

[24] WANG Ying, WANG Bao-feng, XIAO Feng, HUANG Zhen-guo, WANG Yi-jing, RICHARDSON C, CHEN Zhi-xin, JIAO Li-fang, YUAN Hua-tang. Facile synthesis of nanocage Co_3O_4 for advanced lithium-ion batteries [J]. Journal of Power Sources, 2015, 298: 203−208.

[25] LI Li, JIANG Gao-xue, SUN Run-zhi, CAO Bing-qiang. Two-dimensional porous Co_3O_4 nanosheets for high-performance lithium ion batteries [J]. New Journal of Chemistry, 2017, 41: 15283−15288.

[26] JING Lai-ying, KONG Zhen, GUO Fu-an, LIU Xue-hua, FU Ai-ping, LI Mei, LI Hong-liang. Porous structures of carbon-doped Co_3O_4 with tunable morphologies from microflowers to cubes as anodes for high performance

lithium/sodium-ion batteries [J]. Journal of Alloys and Compounds, 2021, 881: 160588.

[27] MULE A R, NARSIMULU D, KAKARLA A K, YU J S. Three-dimensional porous Co_3O_4 hexagonal plates grown on nickel foam as a high-capacity anode material for lithium-ion batteries [J]. Applied Surface Science, 2021, 551: 148942.

[28] CHEN Ming-hua, XIA Xin-hui, YIN Jing-hua, CHEN Qing-guo. Construction of Co_3O_4 nanotubes as high-performance anode material for lithium ion batteries [J]. Electrochimica Acta, 2015, 160: 15−21.

[29] ZHU Yan-fei, CHU Ying-hong, LIANG Jing-hao, LI Yun-sha, YUAN Zi-lin, LI Wen-tao, ZHANG Yi-qiong, PAN Xue-xue, CHOU Shu-lei, ZHAO Ling-zhi, ZENG Rong-hua. Tucked flower-like SnS_2/Co_3O_4 composite for high-performance anode material in lithium-ion batteries [J]. Electrochimica Acta, 2016, 190: 843−851.

[30] WANG Heng-guo, ZHU Yan-jie, YUAN Chen-pei, LI Yan-hui, DUAN Qian. Cobalt-phthalocyanine-derived ultrafine Co_3O_4 nanoparticles as high-performance anode materials for lithium ion batteries [J]. Applied Surface Science, 2017, 414: 398−404.

[31] WANG Li, ZHENG Yao-li, WANG Xiao-hong, CHEN Shou-hui, XU Fu-gang, ZUO Li, WU Jia-feng, SUN Lan-lan, LI Zhuang, HOU Hao-qing, SONG Yong-hai. Nitrogen-doped porous carbon/Co_3O_4 nanocomposites as anode materials for lithium-ion batteries [J]. ACS Applied Materials & Interfaces, 2014, 6: 7117−7125.

[32] LI Jing-fa, XIONG Sheng-lin, LIU Yu-rong, JU Zhi-cheng, QIAN Yi-tai. High electrochemical performance of monodisperse $NiCo_2O_2$ mesoporous microspheres as an anode material for Li-ion batteries [J]. ACS Applied Materials of Interfaces, 2013, 5: 981−988.

改进溶剂热法制备锂离子电池负极材料用多级孔 Co_3O_4 微球

冯 艳[1,2]，曹彩玉[1,2]，曾 婧[3]，王日初[1,2]，彭超群[1,2]，王小锋[1,2]

1. 中南大学 材料科学与工程学院，长沙 410083；
2. 电子封装与先进功能材料湖南省重点实验室，长沙 410083；
3. 中南大学 冶金与环境学院，长沙 410083

摘 要：将溶剂热法与高温煅烧法相结合制备多级孔 Co_3O_4 微球，采用 XRD、SEM、TEM 和电化学测试等技术研究该多级孔 Co_3O_4 微球的结构和性能。结果表明：当煅烧温度为 700 ℃时，所合成的 Co_3O_4(Co_3O_4-700)是由丰富的纳米颗粒(50~200 nm)和大量孔洞(~100 nm)构成的微米级微球(1~2 μm)；该 Co_3O_4-700 负极材料具有优异可逆的充放电容量，表现出最佳的循环性能：在电流密度为 100 mA/g 条件下充放电 100 周后充放电比容量分别为 745 和 755 mA·h/g。

关键词：Co_3O_4；锂离子电池；多孔结构；微球；煅烧

(Edited by Wei-ping CHEN)